frontiers | Frontiers in Neuroscience

TYPE Original Research
PUBLISHED 06 January 2023
DOI 10.3389/fnins.2022.1071272

OPEN ACCESS

EDITED BY
Tie-Qiang Li,
Karolinska University Hospital, Sweden

REVIEWED BY
Yuchi Liu,
University of Michigan, United States
Xin Yu,
Case Western Reserve University, United States

*CORRESPONDENCE
Takayuki Obata
✉ obata.takayuki@qst.go.jp

SPECIALTY SECTION
This article was submitted to Brain Imaging Methods, a section of the journal Frontiers in Neuroscience

RECEIVED 16 October 2022
ACCEPTED 13 December 2022
PUBLISHED 06 January 2023

CITATION
Urushihata T, Takuwa H, Takahashi M, Kershaw J, Shibata S, Nitta N, Tachibana Y, Yasui M, Higuchi M and Obata T (2023) Distribution of intraperitoneally administered deuterium-labeled water in aquaporin-4-knockout mouse brain after middle cerebral artery occlusion.
Front. Neurosci. 16:1071272.
doi: 10.3389/fnins.2022.1071272

Distribution of intraperitoneally administered deuterium-labeled water in aquaporin-4-knockout mouse brain after middle cerebral artery occlusion

Takuya Urushihata[1,2], Hiroyuki Takuwa[1,3], Manami Takahashi[1,3,4], Jeff Kershaw[5], Sayaka Shibata[5], Nobuhiro Nitta[5], Yasuhiko Tachibana[5], Masato Yasui[6], Makoto Higuchi[1] and Takayuki Obata[5]*

[1]Department of Functional Brain Imaging, Institute for Quantum Medical Science, National Institutes for Quantum Science and Technology, Chiba, Japan, [2]Department of Integrative Physiology, Institute of Development, Aging, and Cancer, Tohoku University, Sendai, Japan, [3]Quantum Neuromapping and Neuromodulation Group, Institute for Quantum Life Science, National Institutes for Quantum Science and Technology, Chiba, Japan, [4]Department of Quantum Biology and Molecular Imaging, Tohoku University Graduate School of Medicine, Sendai, Japan, [5]Applied MRI Research, Department of Molecular Imaging and Theranostics, Institute for Quantum Medical Science, National Institutes for Quantum Science and Technology, Chiba, Japan, [6]Department of Pharmacology, Keio University School of Medicine, Keio Advanced Research Center for Water Biology and Medicine, Tokyo, Japan

Introduction: As the movement of water in the brain is known to be involved in neural activity and various brain pathologies, the ability to assess water dynamics in the brain will be important for the understanding of brain function and the diagnosis and treatment of brain diseases. Aquaporin-4 (AQP4) is a membrane channel protein that is highly expressed in brain astrocytes and is important for the movement of water molecules in the brain.

Methods: In this study, we investigated the contribution of AQP4 to brain water dynamics by administering deuterium-labeled water (D_2O) intraperitoneally to wild-type and AQP4 knockout (AQP4-ko) mice that had undergone surgical occlusion of the middle cerebral artery (MCA). Water dynamics in the infarct region and on either side of the anterior cerebral artery (ACA) was monitored with proton-density-weighted imaging (PDWI) performed on a 7T animal MRI.

Results: D_2O caused a negative signal change quickly after administration. The AQP4-ko mice showed a delay of the time-to-minimum in both the contralateral and ipsilateral ACA regions compared to wild-type mice. Also, only the AQP4- ko mice showed a delay of the time-to-minimum in the ipsilateral ACA region compared to the contralateral side. In only the wild-type mice, the signal minimum in the ipsilateral ACA region was higher than that in the contralateral ACA region. In the infarct region, the signal attenuation was slower for the AQP4-ko mice in comparison to the wild-type mice.

Discussion: These results suggest that AQP4 loss affects water dynamics in the ACA region not only in the infarct region. Dynamic PDWI after D_2O administration may be a useful tool for showing the effects of AQP4 *in vivo*.

KEYWORDS

aquaporin-4, brain ischemia, deuterium-labeled water, *in vivo* proton-density-weighted MRI, brain water dynamics

1 Introduction

Water dynamics in the brain has recently been a topic attracting significant interest. Some reports have suggested that water dynamics affects sleep level and dementia (Rasmussen et al., 2018; Taoka and Naganawa, 2020). In previous studies, two-photon microscopy imaging (Iliff et al., 2012) and MRI with an ^{17}O isotope tracer (Kudo et al., 2018) have been used for real-time monitoring of *in vivo* brain water dynamics. However, as two-photon microscopy is invasive and ^{17}O isotope tracers are very expensive, there is a need for a non-invasive, safe, and inexpensive method that can be used to assess and diagnose patients with brain diseases.

Aquaporin is a protein complex embedded in cell membranes that facilitates the exchange of water molecules from one side of the membrane to the other (Vajda et al., 2004; Pavlin et al., 2017; Ohene et al., 2019; Zhang et al., 2019). One subtype, aquaporin-4 (AQP4), is known to express in the end feet of astrocytes. It regulates the flow of water from intravascular and extracellular compartments into the intracellular compartment, and is involved in the removal of excess water in the brain (Badaut et al., 2007b; Verkman, 2009; Rasmussen et al., 2018). AQP4 is known to be involved in many brain diseases such as stroke and dementia (Manley et al., 2000; Aoki et al., 2003; Xu et al., 2015; Zeppenfeld et al., 2017; Abe et al., 2020), and AQP4 knockout (AQP4-ko) animals are often used to investigate the function of AQP4. AQP4-ko mice could be useful for clarifying the role of AQP4 in brain water dynamics and for developing new treatments for brain diseases that target AQP4.

In direct measurements using an optical imaging technique called coherent anti-Stokes Raman scattering (CARS) imaging, and indirect studies using diffusion MRI, different levels of AQP4 expression have been found to affect cell membrane water permeability (Obata et al., 2018). CARS is sensitive to H_2O but is insensitive to deuterium-labeled water (D_2O) signal. Therefore, CARS can be used to observe intracellular and extracellular water exchange after rapid replacement of H_2O with D_2O in the extracellular space. Applying the same procedure during MRI may enable the measurement of water dynamics *in vivo*. Although direct imaging of D_2O with MRI would allow observations to be made with no obfuscating background signal (Obata et al., 1995; Obata et al., 1996), the very low signal is a significant disadvantage. Even at the same concentration as water the D_2O signal would be less than 1% that of ^1H imaging. Investment in a D_2O coil and other specialized equipment would also be necessary. Imaging of the dynamics is instead performed indirectly with proton MRI. Like the case of CARS, it is expected that the process of exchanging H_2O with D_2O will correspond to signal loss in proton-density-weighted imaging (PDWI).

In the early stages of a mouse model of focal cerebral ischemia, it has been reported that the diffusion-weighted imaging (DWI) signal change in AQP4-ko mice is different from that for wild-type mice (Urushihata et al., 2021). Water movement to astrocytes *via* AQP4 is an important process in the early stages of ischemia-induced brain edema formation. AQP4 expression is also sharply increased in ischemic brain edema (De Castro Ribeiro et al., 2006; Hirt et al., 2009), and AQP4-ko or inhibitor administration has been shown to be effective in reducing cellular edema (Manley et al., 2000; Igarashi et al., 2011; Akdemir et al., 2014; Yao et al., 2015). Therefore, we have assessed the early stages of focal cerebral ischemia in a mouse model to highlight the effects of AQP4 on water dynamics. In this study, dynamic PDWI was performed after intraperitoneal administration of D_2O to compare the distribution of water in wild-type and AQP4-ko mice brains after middle cerebral artery occlusion (MCAO).

2 Materials and methods

2.1 Animal preparation

A total of five C57BL/6J wild-type mice (both male and female, 20–30 g, 8–10 weeks; Japan SLC, Hamamatsu, Japan), and six AQP4-ko mice (both male and female, 20–30 g, 8–10 weeks) generated as described previously (Ikeshima-Kataoka et al., 2013; Kato et al., 2014) (acc. no. CDB0758 K),[1] were used in the MRI experiments. All mice were housed individually in separate cages with water and food *ad libitum*. The cages were kept at a temperature of 25°C in a 12-h light/dark cycle. Overall, no clear differences in body weight and size were observed for

1 http://www.cdb.riken.jp/arg/mutant%20mice%20list.html

any of the mice. MCAO was performed for all animals at 3 h before beginning the dynamic PDWI scans. The occlusion was performed using the Tamura method (Tamura et al., 1981), where a permanent occlusion is made at the proximal branch of the MCA in the left cerebral cortex. In this animal model, ischemia in the MCA region occurs soon after MCAO, and the infarction expands and peaks at 24 h after surgery (Tamura et al., 1981; Brint et al., 1988; Garcia et al., 1993; McCullough and Liu, 2011). All experiments were performed in accordance with the institutional guidelines on humane care and use of laboratory animals, and were approved by the Institutional Committee for Animal Experimentation of the National Institutes for Quantum Science and Technology (QST).

2.2 Magnetic resonance imaging measurements

Magnetic resonance imaging measurements were performed with a 7T animal MRI (Bruker BioSpin, Ettlingen, Germany). The mice were initially anesthetized with 3.0% isoflurane (Escain, Mylan Japan, Tokyo, Japan), and then with 1.5–2.0% isoflurane and a 1:5 oxygen/room-air mixture during the MRI experiments. Rectal temperature was continuously monitored with an optical fiber thermometer (FOT-L, FISO, Quebec, QC, Canada), and maintained at 37.0 ± 0.5°C using a heated water pad. Warm air was provided with a homemade automatic heating system regulated by an electric temperature controller (E5CN, Omron, Kyoto, Japan) throughout all experiments. During MRI scanning, the mice lay in a prone position on a MRI-compatible cradle and were held in place with handmade ear bars.

At the beginning of the scanning session, T2-weighted images were acquired with a rapid acquisition with relaxation enhancement (RARE) sequence (TR = 3 s, effective TE = 12 ms, RARE factor = 8, NEX = 1, FOV = 19.2 mm × 19.2 mm, matrix size = 192 × 192, spatial resolution = 0.1 mm × 0.1 mm, slices = 20, slice thickness = 0.75 mm, dummy scans = 2). Subsequently, DWI with a four-shot pulsed-gradient spin-echo (PGSE) echo planar imaging (EPI) sequence (TR = 3 s, TE = 115 ms, matrix size = 128 × 128, spatial resolution = 0.2 mm × 0.2 mm, slices = 3, slice thickness = 1.5 mm, gradient directions = 3, b = 1,000 s/mm^2, Δ = 100 ms, δ = 7 ms) was taken to verify ischemic changes. The central DWI slice corresponded to the T2-weighted image with the largest infarct area, and the DWI confirmed this. Dynamic PDWI was performed using a four-shot spin-echo EPI sequence (TR = 5 s, TE = 11 ms, FOV = 19.2 mm × 19.2 mm, matrix size = 64 × 64, slices = 13, slice thickness = 1 mm) to acquire an image every 20 s for 30 min (total 90 scans). The central PDWI slice was positioned at the same location as the central DWI slice. Region-of-interest (ROI) analysis was

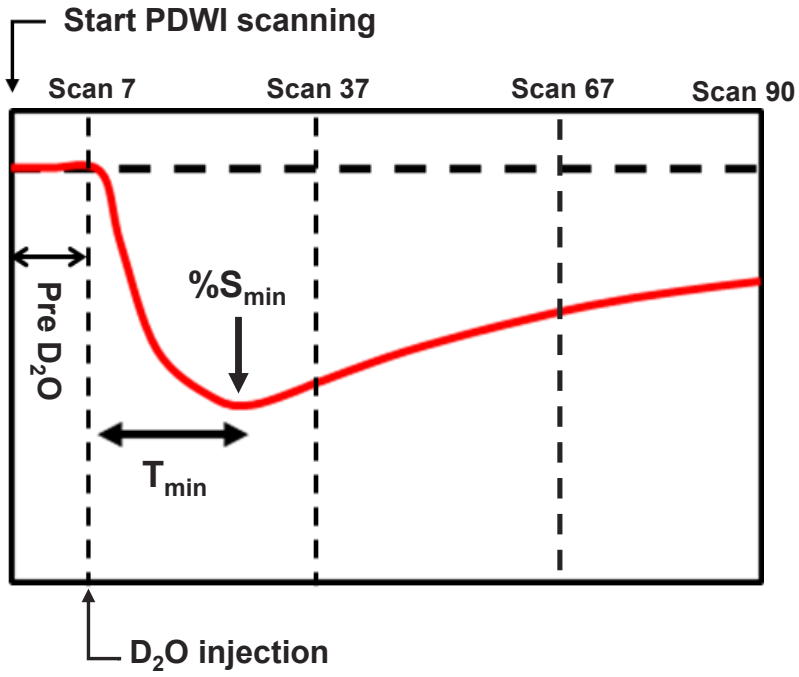

FIGURE 1
Schematic defining the timing of deuterium-labeled water (D_2O) administration in comparison to the proton-density-weighted imaging (PDWI). PDWI images were acquired every 20 s for 30 min (90 scans total). Two min after scanning started, D_2O was administered intraperitoneally. T_{min} indicates the time from administration to the signal minimum.

always performed on the central PDWI slice. Two minutes after scanning began, 1 ml of 99.8% D_2O saline was administered intraperitoneally over 20 s (**Figure 1**). One problem for the administration of D_2O to mice is the very small blood volume of a mouse (2–3 ml). The circulation system would be severely affected (Kselíková et al., 2019) if an intravenous injection of 1 ml D_2O was performed. To avoid this problem, the D_2O was administered intraperitoneally so that the exchange between D_2O and intravascular H_2O is less dramatic.

2.3 PDWI data processing

2.3.1 Signal normalization for maps and time-intensity curves

Analysis of the PDWI data was performed in MATLAB, version R2019a (MathWorks, Natick, MA, USA). The first scan was always discarded because the PDWI data was acquired without any dummy scans. The next five scans acquired in the first 2 min prior to D_2O administration were averaged and used as the reference image S_0 for the pre-D_2O signal. For all scans thereafter the percent signal change, *%S(t)*, was calculated as,

$$\%S(t) = (S(t) - S_0)/S_0 \quad (1)$$

where *S(t)* is the signal intensity at time *t* (min).

2.3.2 ROI analysis

To evaluate PDWI signal changes after D_2O administration, ROIs were drawn at the following three locations: the high-intensity region near the MCA area on the DWI (Infarct ROI), the cortex in the anterior cerebral artery (ACA) territory on the same side as the MCAO (Ipsi-ACA ROI), and the cortex in the opposite ACA territory (Contra-ACA ROI) (**Figure 2A**). The mean time-dependent signal in each ROI between scan 7 and scan 37 (**Figure 1**) after D_2O administration was interpolated with an 8th order polynomial. The time from D_2O administration to the signal minimum ($\%S_{min}$) was defined as the time-to-minimum (T_{min}). Since the transfer rate of D_2O from the peritoneal cavity to the blood is different for different individuals, the following standardization of the signal was performed.

$$\overline{S}_{region}(t) = -\%S_{region}(t)/\%S_{min,ContraACA} \quad (2)$$

where "region" corresponds to one of the ROIs (i.e., Infarct, Ipsi-ACA, or Contra-ACA), and $\%S_{min,ContraACA}$ is the minimum of *%S(t)* for the Contra-ACA ROI. After this procedure, the average value before D_2O administration is zero for all ROIs, and the minimum value of the Contra-ACA signal [$\overline{S}_{contraACA}(t)$] is −1.

For the infarct ROI, a signal minimum was never reached for 8 of the 10 subjects so, as an alternative method to characterize signal change, the slope α of the time-intensity curve between 3 and 5 min after D_2O (3–5 min) was estimated.

2.4 Statistical analysis

Statistical analyses were performed with the Statistics and Machine Learning Toolbox of MatLab. All results are presented as mean ± standard deviation over animals. Student's unpaired *t*-test was used to compare T_{min} and α between mouse genotypes, while the paired *t*-test was used to compare between regions. The normality of each data set was confirmed with the Kolmogorov–Smirnov test. A p-value < 0.05 was interpreted as being statistically significant.

3 Results

3.1 Dynamic PDWI after intraperitoneal D_2O injection

In the DWI performed prior to dynamic PDWI, all mice showed a high signal region in the ipsilateral MCA territory (infarct region in **Figures 2A, D**). PDWI signal decreases in the brain were observed for all mice immediately after intraperitoneal administration (**Figures 2B, C, E, F**), which reflects the transfer of D_2O into the brain. For the wild-type mice, signal change in the Ipsi-ACA ROI was similar to that observed in the Contra-ACA ROI (**Figure 2G**), whereas for the AQP4-ko mice the signal from the Ipsi-ACA ROI appears to be slightly delayed in comparison to that from the Contra-ACA ROI (**Figure 2H**). The signal from the infarct ROI was substantially different in comparison to the other ROIs for both mouse types (**Figures 2G, H**).

3.2 Time-to-minimum (T_{min}) and signal change in the infarct ROI

Figure 3A shows that there was no difference in T_{min} between the Contra-ACA ROI (mean ± std dev = 4.08 ± 0.60) and Ipsi-ACA ROI (4.46 ± 0.83) for the wild-type mice, while for the AQP4-ko mice a significant difference was observed (Contra-ACA ROI: 6.21 ± 1.91; Ipsi-ACA ROI: 11.0 ± 3.65). T_{min} between mouse type was also compared and there were also significant differences in the estimates for the Contra-ACA and Ipsi-ACA ROIs, although the significance was quite weak for the Contra-ACA ROI ($p = 0.028$).

The $\%S_{min}$ was significantly higher in the Ipsi-ACA ROI (−6.00 ± 1.12) than in the Contra-ACA ROI (−6.16 ± 1.02) for the wild-type mice (**Figure 3B**). There was no significant difference in the corresponding comparison for the AQP4-ko mice (Ipsi-ACA ROI: −7.74 ± 1.61; Contra-ACA ROI: −7.48 ± 0.85). When comparing the $\%S_{min}$ between genotypes, the Ipsi-ACA ROI had a significantly higher value for the wild-type mice.

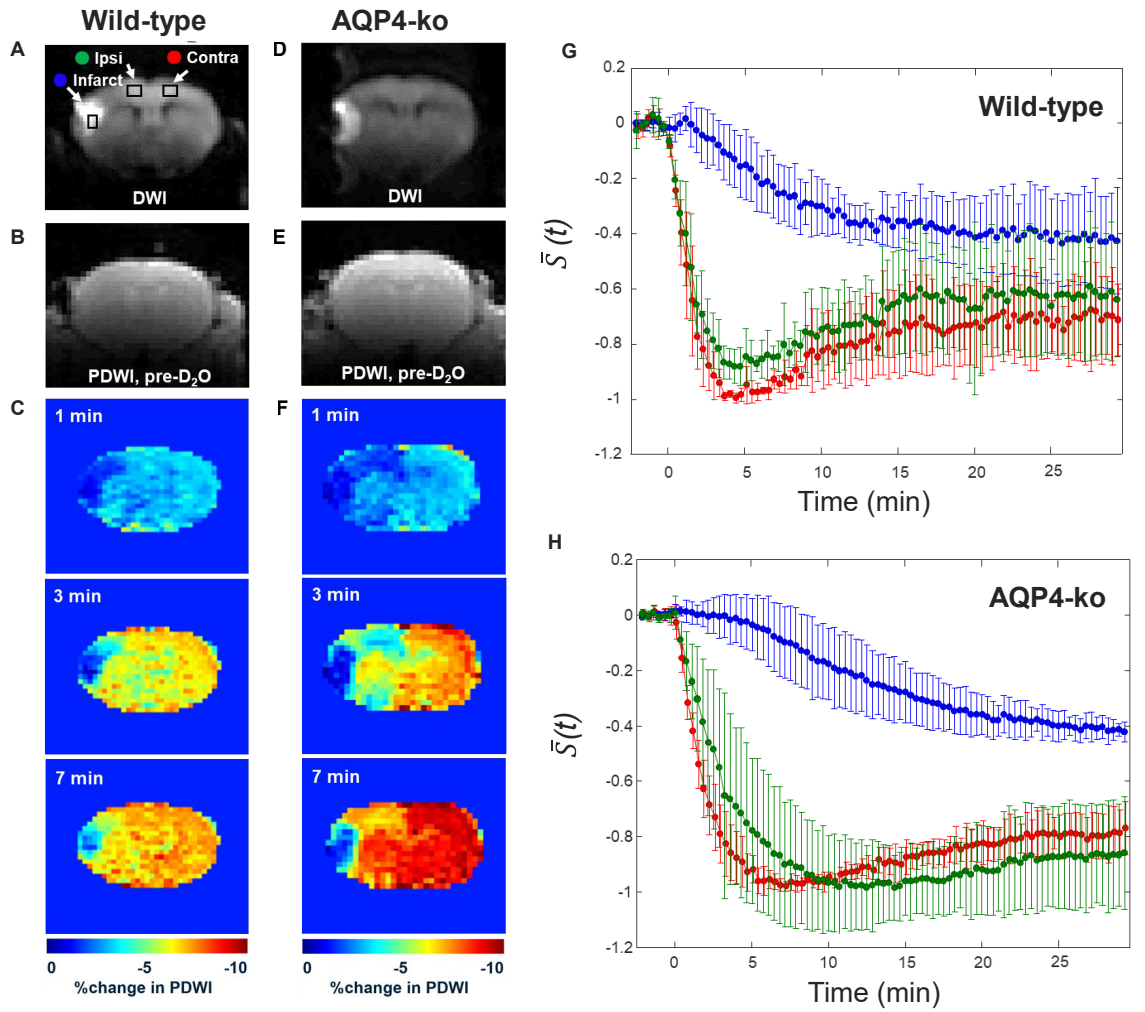

FIGURE 2
Water dynamics measurements after intraperitoneal administration of deuterium-labeled water (D_2O). **(A–C)** Representative diffusion-weighted imaging (DWI) images, pre-D_2O baseline proton-density-weighted imaging (PDWI) images and % signal change at 1, 3, and 7 min after D_2O administration for the wild-type mice. **(D–F)** A similar set of images for the AQP4 knockout (AQP4-ko) mice. **(G)** Standardized signal changes in each region-of-interest (ROI) for the wild-type mice. **(H)** Standardized signal changes in each ROI for the AQP4-ko mice. Error bars indicate standard deviations across animals. The Infarct (blue), Ipsi-anterior cerebral artery (ACA) (green), and Contra-ACA (red) ROIs are shown on the DWI image in panel **(A)**.

Since the data did not reach a minimum in the infarct ROI for 8 out of the 11 mice, the slope α of the signal attenuation at 3–5 min after D_2O administration was used to evaluate signal change (Figure 4A). For the wild-type mice α was -0.016 ± 0.007/min, which was smaller than the α of -0.004 ± 0.006/min for the AQP4-ko mice. This difference was significant ($p = 0.015$; Figure 4B).

4 Discussion

In this experiment, we used dynamic PDWI after an intraperitoneal D_2O injection to observe the biodistribution in brains with MCAO. Our method depicted the AQP4-expression-related temporal and spatial differences in water dynamics associated with focal cerebral ischemia. Significant differences in the PDWI signal change were observed between wild-type and AQP4-ko mice.

Deuterium is a stable isotope of hydrogen, and D_2O is non-toxic unless in high volumes (Kselíková et al., 2019). Since D_2O is undetectable in ^1H MRI, its mixing with H_2O *in vivo* causes concentration-dependent attenuation of the PDWI signal. So D_2O is effectively a negative contrast agent. The motion of D_2O *in vivo* is the same as H_2O so it can pass through AQPs (Obata et al., 2018), making it a potential means to assess AQP function and perfusion. D_2O was administered intraperitoneally in the present study because of the possibility that intravenous administration of a high volume of D_2O might affect the

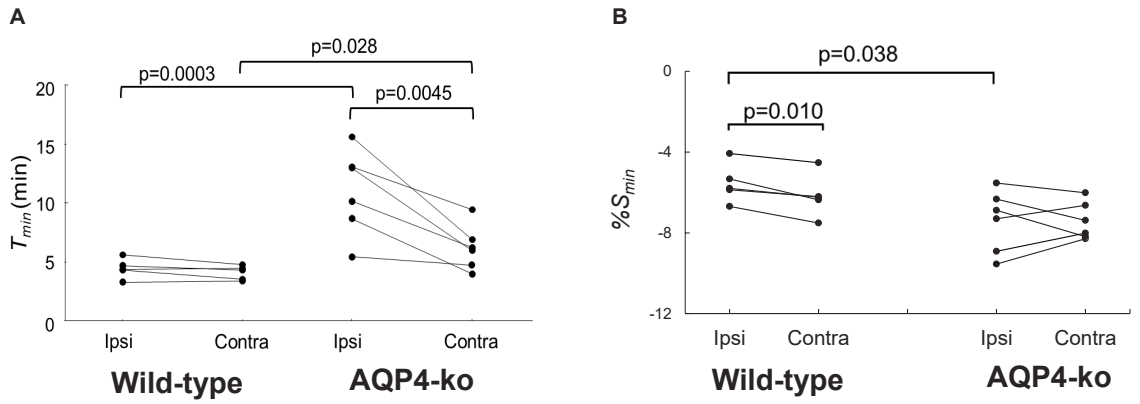

FIGURE 3
Comparisons of the time-to-min (T_{min}) and signal minimum ($\%S_{min}$) in the anterior cerebral artery (ACA) regions-of-interest (ROIs) after deuterium-labeled water (D_2O) administration. **(A)** T_{min} for the wild-type (n = 5) and AQP4 knockout (AQP4-ko) (n = 6) mice. **(B)** $\%S_{min}$ for both mouse genotypes. Results for the same animal are connected by lines. Comparisons between genotypes were made using an unpaired t-test, while the comparison between the ipsi and contralateral sides were made with a paired t-test. The resulting p values are shown at the top of the figure. Note that, although the data from five the wild-type mice are plotted, the data for two of the animals nearly overlap so that it appears that there is only four data points.

cardiovascular system (Kselíková et al., 2019). Comparison of intraperitoneal and intravenous administration of Evans blue to evaluate blood brain barrier (BBB) permeability has been reported to show no difference in brain accumulation at any time point (Manaenko et al., 2011). The same is probably true for D_2O, which easily passes through the BBB. Intraperitoneal administration was suitable for D_2O imaging because it causes less damage to the body and allows experiments to be repeated.

4.1 Time-to-minimum (T_{min}) and signal-at-min ($\%S_{min}$)

There was no significant difference in T_{min} between the ipsilateral and contralateral sides for the wild-type mice, while for the AQP4-ko mice the value was significantly larger on the ipsi side (**Figure 3**). This means that changes to the signal in the Ipsi-ACA ROI of the AQP-ko mice was delayed. In general, when ligation is performed at the main trunk of the MCA, arterial blood is partially compensated by flow from the ACA, which means that supply to the ACA region is reduced (Dziennis et al., 2015). The elongation of T_{min} for the Ipsi-ACA ROI of the AQP4-ko mice seems to be naturally affected by this cerebral blood flow (CBF) reduction. The fact that there was no significant change for the wild-type mice is curious. It is possible that the number of active AQP4 sites increases in the Ipsi-ACA region of the wild-type mice so that the water transfer to brain is maintained even under the condition of low CBF (Badaut et al., 2007a).

For T_{min}, there was a significant difference between the wild-type and AQP4-ko mice even in the Contra-ACA. This may be due to the delayed flow of water from the capillary to the perivascular space (Mestre et al., 2020) and the enlargement of the extracellular space, as suggested by diffusion MRI studies (Urushihata et al., 2021).

The $\%S_{min}$ in the Ipsi-ACA ROIs of the wild-type mice was higher than that in the Contra-ACA ROIs for all animals (**Figure 3B**). As there was no difference in T_{min} for these ROIs, the concentration of D_2O in the Ipsi-ACA area was about 12% less than that in the Contra-ACA region. This suggests that dispersion of the D_2O is slightly reduced due to the MCAO even in the wild-type mice. On the other hand, there was no difference between the $\%S_{min}$ of the Ipsi-ACA ROIs and Contra-ACA ROIs for the AQP4-ko mice (**Figure 3B**). This may be due to the signal reduction by D_2O influx to the enlarged extracellular space, which may cancel the $\%S_{min}$ change as seen in the wild-type mice. The wild-type mice had a significantly higher $\%S_{min}$ than the AQP4-ko mice for the Ipsi-ACA ROI, but the reason for this is unclear.

4.2 Signal change in the infarct area

Signal attenuation in the infarct area tended to be slower for the AQP4-ko mice. The infarct region is thought to have almost no blood flow for both the wild-type and AQP4-ko mice due to the MCAO. Since AQP4 expression is known to increase rapidly after occlusion in the core and border regions of the lesion (De Castro Ribeiro et al., 2006; Hirt et al., 2009), the difference in signal changes in the infarct ROI may be due to the faster inflow of D_2O from the surrounding intact area in the wild-type mice. This mechanism may be related to the larger influx of water from surrounding tissue to the infarct lesion *via* the perivascular space in the wild-type mice (Mestre et al., 2020).

The infarct area on the DWI was on average slightly larger for the APQ4-ko mice, but there was no indication that

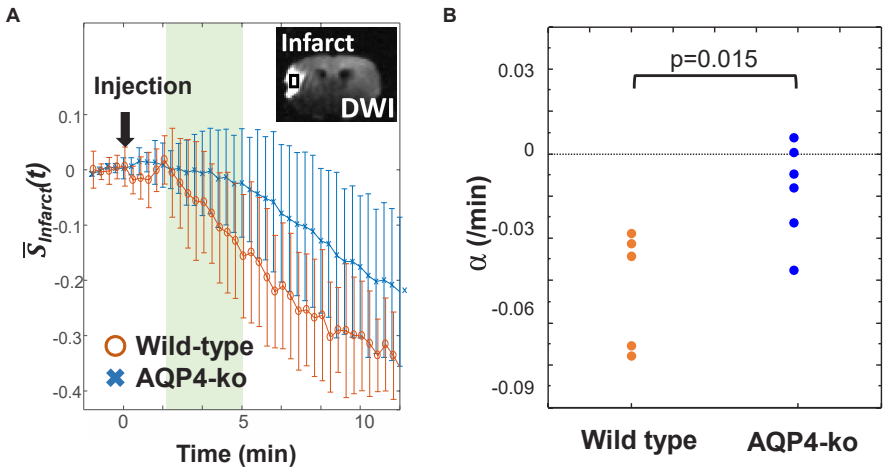

FIGURE 4
Signal attenuation in the infarct region. **(A)** Standardized proton-density-weighted imaging (PDWI) signal in the infarct region of the wild-type (orange) and AQP4 knockout (AQP4-ko) (blue) mice. The slope α is calculated from the signal recorded at 3–5 min after deuterium-labeled water (D_2O) injection. **(B)** The estimates of α for the two groups were compared using an unpaired *t*-test and the *p* value is shown at the top of the figure.

the condition of the AQP4-ko animals after MCAO differed significantly from the wild-type mice. In an earlier study that used the same mouse genotypes and techniques as used here, it was found that the apparent diffusion coefficient (ADC) in the ischemic area of the AQP4-ko mice is lower than that for the wild-type mice (Urushihata et al., 2021). So, AQP4-ko clearly affects water diffusion in the ischemic area. However, no evidence was found to confirm reports that AQP4-ko reduces the size of the affected area on DWI after stroke (e.g., Manley et al., 2000).

4.3 Limitation

Since the arterial input function was not measured in this study, the possibility remains that blood D_2O levels may differ between genotypes. However, a previous study reported that AQP4-ko mice do not differ from wild-type mice in spontaneous isosmotic fluid absorption from the abdominal cavity (Yang et al., 1999). Also, the finding that D_2O dynamics in the brain differed between the healthy and injured side of the same genotype is unaffected by D_2O uptake from the peritoneal cavity because the absorption condition is the same for both sides.

5 Conclusion

Dynamic PDWI after administration of D_2O is useful for investigating the dynamics of water in the brain and is thought to be effective in showing the effects of AQP4. Under severe ischemic conditions, the differences between the wild-type and AQP4-ko mice were significant. This may be because some compensation mechanism for intracerebral water transfer fails for AQP4-ko mice in a pathological state.

Data availability statement

The raw data supporting the conclusions of this article will be made available by the authors, without undue reservation.

Ethics statement

The animal study was reviewed and approved by the Institutional Committee for Animal Experimentation of the National Institutes for Quantum Science and Technology.

Author contributions

TU: conceptualization, data curation, formal analysis, investigation, methodology, project administration, software, visualization, and writing – original draft. HT: conceptualization, investigation, and writing – review and editing. MT, SS, and NN: investigation and writing – review and editing. JK: methodology and writing – original draft. YT: methodology and writing – review and editing. MY: resources and writing – review and editing. MH: supervision and writing – review and editing. TO: conceptualization, funding acquisition, methodology, project administration, software, supervision, and writing – original

draft. All authors contributed to the article and approved the submitted version.

Funding

This work was supported by a Grant-in-aid for Scientific Research (KAKENHI, #15H04910 [TO]) from the Japan Society for the Promotion of Science (JSPS).

Acknowledgments

We thank Takeharu Minamihisamatsu for help with animal management.

Conflict of interest

The authors declare that the research was conducted in the absence of any commercial or financial relationships that could be construed as a potential conflict of interest.

Publisher's note

References

Abe, Y., Ikegawa, N., Yoshida, K., Muramatsu, K., Hattori, S., Kawai, K., et al. (2020). Behavioral and electrophysiological evidence for a neuroprotective role of aquaporin-4 in the 5xFAD transgenic mice model. *Acta Neuropathol. Commun.* 8:67. doi: 10.1186/s40478-020-00936-3

Akdemir, G., Ratelade, J., Asavapanumas, N., and Verkman, A. S. (2014). Neuroprotective effect of aquaporin-4 deficiency in a mouse model of severe global cerebral ischemia produced by transient 4-vessel occlusion. *Neurosci. Lett.* 574, 70–75. doi: 10.1016/j.neulet.2014.03.073

Aoki, K., Uchihara, T., Tsuchiya, K., Nakamura, A., Ikeda, K., and Wakayama, Y. (2003). Enhanced expression of aquaporin 4 in human brain with infarction. *Acta Neuropathol.* 106, 121–124. doi: 10.1007/s00401-003-0709-y

Badaut, J., Brunet, J.-F., and Regli, L. (2007b). Aquaporins in the brain: From aqueduct to "multi-duct." *Metab. Brain Dis.* 22, 251–263. doi: 10.1007/s11011-007-9057-2

Badaut, J., Ashwal, S., Tone, B., Regli, L., Tian, H. R., and Obenaus, A. (2007a). Temporal and regional evolution of aquaporin-4 expression and magnetic resonance imaging in a rat pup model of neonatal stroke. *Pediatr. Res.* 62, 248–254. doi: 10.1203/pdr.0b013e3180db291b

Brint, S., Jacewicz, M., Kiessling, M., Tanabe, J., and Pulsinelli, W. (1988). Focal brain ischemia in the rat: Methods for reproducible neocortical infarction using tandem occlusion of the distal middle cerebral and ipsilateral common carotid arteries. *J. Cereb. Blood Flow Metab.* 8, 474–485. doi: 10.1038/jcbfm.1988.88

De Castro Ribeiro, M., Hirt, L., Bogousslavsky, J., Regli, L., and Badaut, J. (2006). Time course of aquaporin expression after transient focal cerebral ischemia in mice. *J. Neurosci. Res.* 83, 1231–1240. doi: 10.1002/jnr.20819

Dziennis, S., Qin, J., Shi, L., and Wang, R. K. (2015). Macro-to-micro cortical vascular imaging underlies regional differences in ischemic brain. *Sci. Rep.* 5:10051. doi: 10.1038/srep10051

Garcia, J. H., Yoshida, Y., Chen, H., Li, Y., Zhang, Z. G., Lian, J., et al. (1993). Progression from ischemic injury to infarct following middle cerebral artery occlusion in the rat. *Am. J. Pathol.* 142, 623–635.

Hirt, L., Ternon, B., Price, M., Mastour, N., Brunet, J. F., and Badaut, J. (2009). Protective role of early aquaporin 4 induction against postischemic edema formation. *J. Cereb. Blood Flow Metab.* 29, 423–433. doi: 10.1038/jcbfm.2008.133

Igarashi, H., Huber, V. J., Tsujita, M., and Nakada, T. (2011). Pretreatment with a novel aquaporin 4 inhibitor, TGN-020, significantly reduces ischemic cerebral edema. *Neurol. Sci.* 32, 113–116. doi: 10.1007/s10072-010-0431-1

Ikeshima-Kataoka, H., Abe, Y., Abe, T., and Yasui, M. (2013). Immunological function of aquaporin-4 in stab-wounded mouse brain in concert with a pro-inflammatory cytokine inducer, osteopontin. *Mol. Cell. Neurosci.* 56, 65–75. doi: 10.1016/j.mcn.2013.02.002

Iliff, J. J., Wang, M., Liao, Y., Plogg, B. A., Peng, W., Gundersen, G. A., et al. (2012). A paravascular pathway facilitates CSF flow through the brain parenchyma and the clearance of interstitial solutes, including amyloid β. *Sci. Transl. Med.* 4:147ra111. doi: 10.1126/SCITRANSLMED.3003748

Kato, J., Takai, Y., Hayashi, M. K., Kato, Y., Tanaka, M., Sohma, Y., et al. (2014). Expression and localization of aquaporin-4 in sensory ganglia. *Biochem. Biophys. Res. Commun.* 451, 562–567. doi: 10.1016/j.bbrc.2014.08.026

Kselíková, V., Vítová, M., and Bišová, K. (2019). Deuterium and its impact on living organisms. *Folia Microbiol.* 64, 673–681. doi: 10.1007/S12223-019-00740-0

Kudo, K., Harada, T., Kameda, H., Uwano, I., Yamashita, F., Higuchi, S., et al. (2018). Indirect proton MR imaging and kinetic analysis of 17 O-labeled water tracer in the brain. *Magn. Reson. Med. Sci.* 17, 223–230. doi: 10.2463/MRMS.MP.2017-0094

Manaenko, A., Chen, H., Kammer, J., Zhang, J. H., and Tang, J. (2011). Comparison Evans Blue injection routes: Intravenous vs. intraperitoneal, for measurement of blood-brain barrier in a mice hemorrhage model. *J. Neurosci. Methods* 195, 206–210. doi: 10.1016/J.JNEUMETH.2010.12.013

Manley, G. T., Fujimura, M., Ma, T., Noshita, N., Filiz, F., Bollen, A. W., et al. (2000). Aquaporin-4 deletion in mice reduces brain edema after acute water intoxication and ischemic stroke. *Nat. Med.* 6, 159–163. doi: 10.1038/72256

McCullough, L. D., and Liu, F. (2011). Middle cerebral artery occlusion model in rodents: Methods and potential pitfalls. *J. Biomed. Biotechnol.* 2011:464701. doi: 10.1155/2011/464701

Mestre, H., Du, T., Sweeney, A. M., Liu, G., Samson, A. J., Peng, W., et al. (2020). Cerebrospinal fluid influx drives acute ischemic tissue swelling. *Science* 367:eaax7171. doi: 10.1126/science.aax7171

Obata, T., Ikehira, H., Koga, M., Yoshida, K., Kimura, F., and Tateno, T. (1995). Deuterium magnetic resonance imaging of rabbit eye in vivo. *Magn. Reson. Med.* 33, 569–572. doi: 10.1002/mrm.1910330417

Obata, T., Ikehira, H., Ueshima, Y., Kato, H., Koga, M., and Yoshida, K. (1996). Noninvasive analysis of water movement in rat testis using deuterium magnetic resonance imaging. *Magn. Reson. Imaging* 14, 115–119. doi: 10.1016/0730-725x(95)02038-u

Obata, T., Kershaw, J., Tachibana, Y., Miyauchi, T., Abe, Y., Shibata, S., et al. (2018). Comparison of diffusion-weighted MRI and anti-Stokes Raman scattering (CARS) measurements of the inter-compartmental exchange-time of water in expression-controlled aquaporin-4 cells. *Sci. Rep.* 8:17954. doi: 10.1038/s41598-018-36264-9

Ohene, Y., Harrison, I. F., Nahavandi, P., Ismail, O., Bird, E. V., Ottersen, O. P., et al. (2019). Non-invasive MRI of brain clearance pathways using multiple echo time arterial spin labelling: An aquaporin-4 study. *Neuroimage* 188, 515–523. doi: 10.1016/j.neuroimage.2018.12.026

Pavlin, T., Nagelhus, E. A., Brekken, C., Eyjolfsson, E. M., Thoren, A., Haraldseth, O., et al. (2017). Loss or mislocalization of aquaporin-4 affects diffusion properties and intermediary metabolism in gray matter of mice. *Neurochem. Res.* 42, 77–91. doi: 10.1007/s11064-016-2139-y

Rasmussen, M. K., Mestre, H., and Nedergaard, M. (2018). The glymphatic pathway in neurological disorders. *Lancet. Neurol.* 17, 1016–1024. doi: 10.1016/S1474-4422(18)30318-1

Tamura, A., Graham, D. I., McCulloch, J., and Teasdale, G. M. (1981). Focal cerebral ischaemia in the rat: I. Description of technique and early neuropathological consequences following middle cerebral artery occlusion. *J. Cereb. Blood Flow Metab.* 1, 53–60. doi: 10.1038/jcbfm.1981.6

Taoka, T., and Naganawa, S. (2020). Neurofluid dynamics and the glymphatic system: A neuroimaging perspective. *Korean J. Radiol.* 21, 1199–1209. doi: 10.3348/KJR.2020.0042

Urushihata, T., Takuwa, H., Takahashi, M., Kershaw, J., Tachibana, Y., Nitta, N., et al. (2021). Exploring cell membrane water exchange in aquaporin-4-deficient ischemic mouse brain using diffusion-weighted MRI. *Eur. Radiol. Exp.* 5:45. doi: 10.1186/S41747-021-00244-Y/TABLES/2

Vajda, Z., Pedersen, M., Doczi, T., Sulyok, E., and Nielsen, S. (2004). Studies of mdx mice. *Neuroscience* 129, 991–996. doi: 10.1016/J.NEUROSCIENCE.2004.08.055

Verkman, A. S. (2009). Knock-out models reveal new aquaporin functions. *Handb. Exp. Pharmacol.* 190, 359–381. doi: 10.1007/978-3-540-79885-9_18

Xu, Z., Xiao, N., Chen, Y., Huang, H., Marshall, C., Gao, J., et al. (2015). Deletion of aquaporin-4 in APP/PS1 mice exacerbates brain Aβ accumulation and memory deficits. *Mol. Neurodegener.* 10:58. doi: 10.1186/s13024-015-0056-1

Yang, B., Folkesson, H. G., Yang, J., Mattick, L. R., Ma, T., and Verkman, A. S. (1999). Reduced osmotic water permeability of the peritoneal barrier in aquaporin-1 knockout mice. *Am. J. Physiol.* 276, C76–C81. doi: 10.1152/ajpcell.1999.276.1.C76

Yao, X., Derugin, N., Manley, G. T., and Verkman, A. S. (2015). Reduced brain edema and infarct volume in aquaporin-4 deficient mice after transient focal cerebral ischemia. *Neurosci. Lett.* 584, 368–372. doi: 10.1016/j.neulet.2014.10.040

Zeppenfeld, D. M., Simon, M., Haswell, J. D., D'Abreo, D., Murchison, C., Quinn, J. F., et al. (2017). Association of perivascular localization of aquaporin-4 with cognition and Alzheimer disease in aging brains. *JAMA Neurol.* 74, 91–99. doi: 10.1001/jamaneurol.2016.4370

Zhang, Y., Xu, K., Liu, Y., Erokwu, B. O., Zhao, P., Flask, C. A., et al. (2019). Increased cerebral vascularization and decreased water exchange across the blood-brain barrier in aquaporin-4 knockout mice. *PLoS One* 14:e0218415. doi: 10.1371/journal.pone.0218415